

Photocatalytic Degradation of Acid Blue and Brilliant Yellow Dyes in Visible Light: A Comparative Study over Nano TiO₂ and La₂O₃-TiO₂ Nano Composites

Vasantham Amrutha^{1,2}, Vijayalaxmi Burri¹, Sajeeda Mohammed¹, Ravali Bingi¹, Venkatesham Kothabai¹, Padma Bukya¹ and Hari Padmasri Aytam^{1*}

¹Department of Chemistry, Osmania University, Hyderabad-500 007, Telangana, India.

²Department of Chemistry, Government City College, Nayapul, Hyderabad, Telangana, India

Abstract:

The utilization of titanium dioxide (TiO₂) in environmental remediation is promising due to its photocatalytic properties. This study focuses on creating La-doped TiO₂ nanocomposite through the sol-gel method, showcasing its strong photocatalytic capability. In contrast to pure TiO₂ nanoparticles, a 5wt % La³⁺-doped titania nanocomposite exhibited exceptional photocatalytic performance. The nanocomposites underwent comprehensive analysis, including X-ray diffraction (XRD), Nitrogen physisorption (BET), Scanning Electron Microscopy (SEM) with Extended X-ray Diffraction (EDAX), UV-Vis, Photoluminescence (PL) and X-ray Photoelectron Spectroscopy (XPS). XRD patterns indicated that both pristine and La₂O₃-TiO₂ materials formed tetragonal structures with an anatase phase. The band-edge potential of TiO₂ for degradation was suitably modified by La₂O₃ doping, as inferred from calculated band-edge positions. UV-Vis spectra revealed varying E_g values, transitioning from 3.12 eV for pure titania to 2.75 eV La doping. Remarkably, these materials demonstrated significant photocatalytic prowess, achieving 99% degradation of Acid Blue dye and 96% for Brilliant Yellow dye after 180 minutes under visible light irradiation.

Keywords: Nanocomposite, La₂O₃, Photocatalytic degradation, Sol-gel, XRD, SEM, PL, XPS, doping

Date of Submission: 27-08-2023

Date of Acceptance: 07-09-2023

I. INTRODUCTION

Extensive research has been conducted over the past few decades on semiconductor-mediated photocatalytic degradation of organic pollutants. Among these semiconductors, TiO₂ stands out as a highly efficient photocatalyst for pollutant degradation in water, facilitated by the generation of powerful oxidizing agents such as hydroxyl radicals and superoxide radical anions under UV light [1]. Notably, TiO₂'s wide band gap energy (3.2 eV for anatase) limits its excitation to UV light, preventing it from utilizing visible light. To address this, introducing metal or non-metal dopants into the TiO₂ structure can extend its response to visible light [2, 3]. Various methods are employed for TiO₂ doping, including ion implantation, sol-gel, hydrothermal, and solid-state reactions. The sol-gel process, which is cost-effective and offers nanoparticle size and shape control, is particularly favored [4].

The mechanism behind the photocatalytic degradation of pollutants with metal-doped TiO₂ involves introducing a new energy level (dopant impurity level) via dispersed metal nanoparticles in the TiO₂ matrix, creating electron traps. This trapping curbs electron-hole recombination during irradiation, thus prolonging charge carrier lifetimes. Dopants enhance the separation of photo-induced electrons and holes, and they also increase visible light absorption by narrowing the band gap [5].

This paper discusses the synthesis of La-doped TiO₂ nanocomposites using the sol-gel method, followed by characterization using X-ray diffraction (XRD), nitrogen physisorption (BET), scanning electron microscopy (SEM) with Extended X-ray Diffraction (EDAX), UV-Vis, and X-ray photoelectron spectroscopy (XPS). The photocatalysts' performance was evaluated by studying the decolorization of Acid Blue and Brilliant Yellow under visible light sources. La³⁺ ions, acting as p-type dopants, function as electron trappers within the TiO₂ lattice, effectively slowing charge recombination and enhancing photocatalytic activity.

II. EXPERIMENTAL

Synthesis of nano TiO₂ and La-doped TiO₂ photocatalysts:

Synthesis of nano TiO₂ and La-doped TiO₂ photocatalysts was achieved via the sol-gel method. For the Ti-La sample, a solution of titanium (IV) isopropoxide and lanthanum nitrate was prepared to achieve 5.0 wt.%

of La_2O_3 in titania. Three independent solutions (A, B, and C) were prepared, where solution A contained AcOH in ethanol, solution B involved $\text{Ti}(\text{OC}_3\text{H}_7)_4$ dissolved in ethanol, and solution C consisted of $\text{La}(\text{NO}_3)_3 \cdot 5\text{H}_2\text{O}$ in deionized water. The solutions were combined, leading to gel formation, the resulting gel solution underwent further steps, including the addition of aq. NH_3 solution, drying at specific temperatures and calcination in air at 500°C for 4 hours.

Characterization:

Powder X-ray diffraction (XRD) analysis was performed using a Rigaku miniplex powder X-ray diffractometer. Surface properties were measured using N_2 adsorption, and surface morphology was analyzed through field emission scanning electron microscopy (FE-SEM) with Energy Dispersive X-ray (EDX) analysis for element distribution. UV-Vis diffuse reflectance spectra (UV-Vis DRS) were recorded using a JASCO V650 UV-Vis spectrophotometer.

Photo catalytic degradation:

The experiments were carried out on a reactor with visible light irradiation, and the degradation efficiency of Acid blue was measured using absorbance changes. The details of experimental set up are described in our earlier studies [6]. The below formula was used to estimate degradation efficiency.

$$\%D = \frac{C_0 - C}{C_0} \times 100 = \frac{A_0 - A}{A_0} \times 100$$

where C_0 & A_0 are the concentration & absorbance respectively before the reaction and C & A are the concentration & absorbance obtained using centrifugation every 30 min during the reaction.

III. RESULTS AND DISCUSSION

X-Ray Diffraction (XRD):

X-ray diffraction (XRD) results as shown in figure 1 revealed dominant diffraction peaks for TiO_2 nanoparticles corresponding to the anatase phase. La_2O_3 - TiO_2 nanocomposite also exhibited an anatase phase without any additional peaks for La_2O_3 , indicating successful doping. The most intensive diffraction decreased and broadened with lanthanum addition, leading to reduced crystallite size for Ti-La sample compared to pure titania [5].

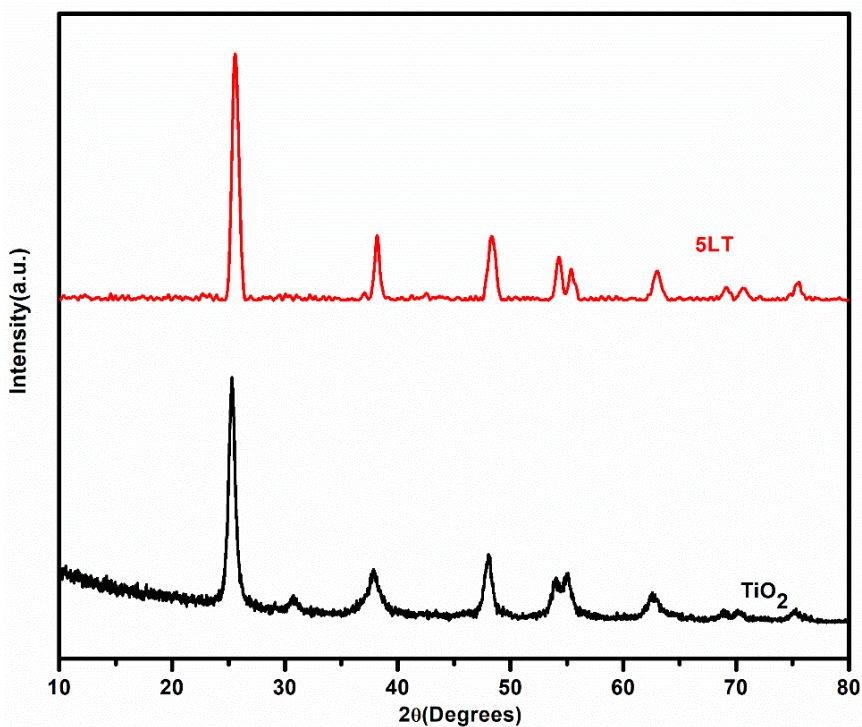


Figure 1: X-ray diffraction patterns of TiO_2 and 5wt% La_2O_3 - TiO_2

BET-Surface Area:

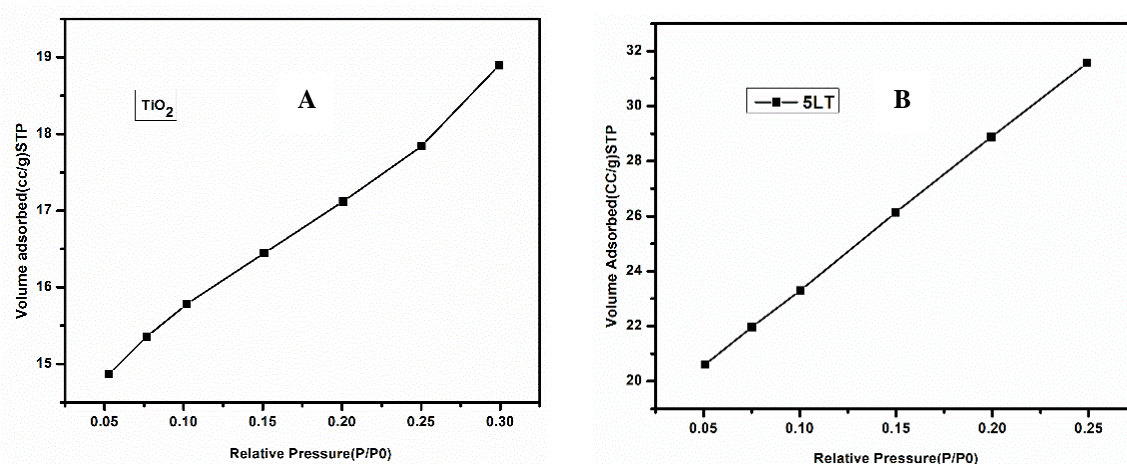


Figure 2: BET-Adsorption Isotherms of (A) Nano TiO₂ and (B) La-doped TiO₂

The BET-surface area of nano titania and 5wt% La₂O₃-TiO₂ were determined to be 57 and 109 m²g⁻¹ respectively, indicating an increase in the specific surface area of TiO₂ due to La doping. The N₂ adsorption-desorption isotherms depicted in figure 2 demonstrated type IV behaviour, with the Ti-La sample presenting type H₂ hysteresis attributed to capillary condensation in mesoporous materials.

UV-DRS:

Both nano TiO₂ and 5wt% La₂O₃-TiO₂ exhibited absorbance between 400-480 nm. Energy of Band gap values were calculated from the Kubelka – Munk Plot to be 2.75 and 3.12 eV for La-doped TiO₂ and nano TiO₂ photocatalysts, respectively. Physico-Chemical Characteristics of Nano photo catalysts are presented in Table 1.

Table 1: Physico-Chemical Characteristics of Nano Photocatalysts

Catalyst	XRD Crystallite Size (nm)	BET-SA (m ² g ⁻¹ cat)	UV-DRS Wavelength of Absorption Edge (nm)	Band Gap Energy (eV)
TiO ₂	8.24	57	390	3.12
5% La ₂ O ₃ -TiO ₂	5.2	109	420	2.75

The UV-vis DRS of pure TiO₂ and La₂O₃-TiO₂ presented in figure 3 showed that La₂O₃-TiO₂ experienced a red shift compared to pure TiO₂. This shift was due to the charge-transfer transition between rare earth ion 4f orbital electrons and the TiO₂ conduction or valence band. La³⁺ doping in titania expanded the absorption range in the visible-light region. The estimated band gap energies (E_g) were 3.12 and 2.75 eV for TiO₂ and La₂O₃-TiO₂, respectively, indicating that the La³⁺ dopant narrowed the band gap of TiO₂, extending the optical response into the visible-light region.

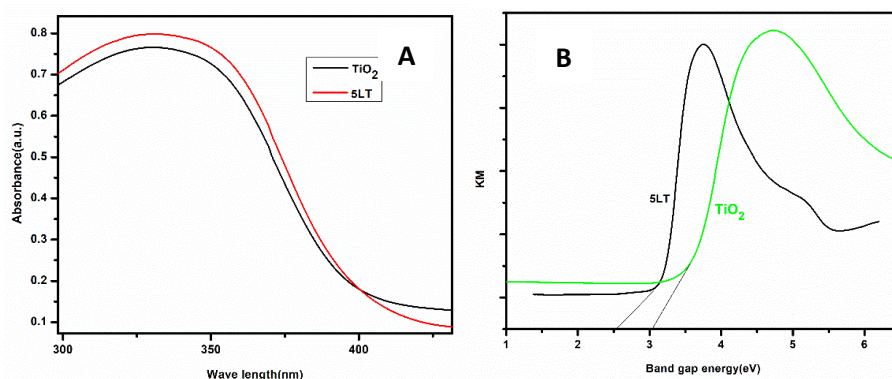


Figure 3: (A) UV-DRS and (B) Kubelka – Munk Plot of Nano TiO_2 and 5% $\text{La}_2\text{O}_3\text{-TiO}_2$

FTIR spectra:

FTIR absorption bands shown in figure 4 in the $680\text{-}860\text{ cm}^{-1}$ range corresponded to vibrational frequencies of Ti-O bonds and the stretching vibrations of Ti-OH and Ti-O bonds. Bands at 1231 , 1375 , and 1740 cm^{-1} were associated with C=O stretching frequency and frequency of C=C bonds stretching organic compounds remained after synthesis. Absorption bands at $2900\text{-}3000$ and 3450 cm^{-1} indicated O-H vibration modes, revealing increased H_2O adsorption on the surface of $\text{La}_2\text{O}_3\text{-TiO}_2$ after La^{3+} doping, leading to greater OH radical production upon light irradiation [9].

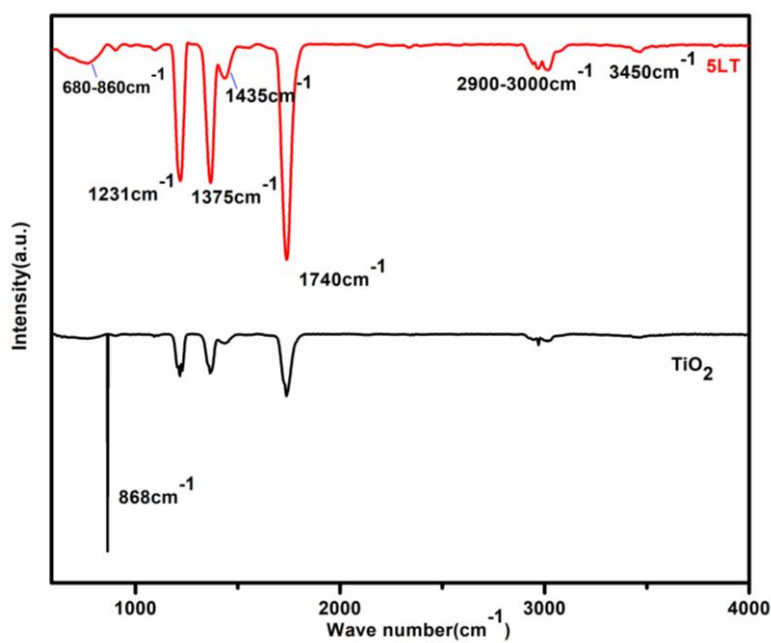


Figure 4: FTIR Spectrum of TiO_2 and 5% $\text{La}_2\text{O}_3\text{-TiO}_2$

Photoluminescence:

Intense PL peaks emerged around 415 nm with reduced emission intensity in La-doped TiO_2 . The intensity of photoluminescence is generally influenced by crystallinity, where materials with higher crystallinity exhibit stronger PL intensity [10].

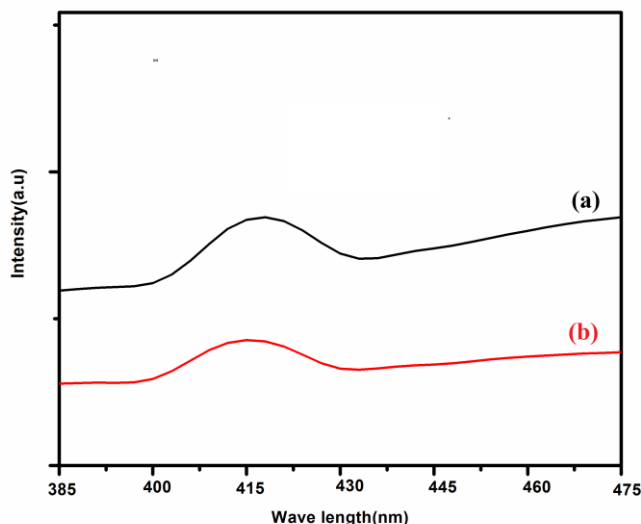


Figure 5: PL Spectra of (a) TiO_2 and (b) $5\% \text{La}_2\text{O}_3\text{-TiO}_2$

Figure 5 illustrates the fluorescence spectra (PL) of both pure and La-doped TiO_2 samples. This observation suggests that La doping can slow down the radiative recombination process of photogenerated electrons and holes in TiO_2 . This effect could stem from the introduction of new defect sites or recombination centers that enhance the recombination of photogenerated electrons and holes. The photoluminescence measurements provide evidence that lower intensity in the PL spectrum corresponds to higher photocatalytic activity.

SEM-EDAX:

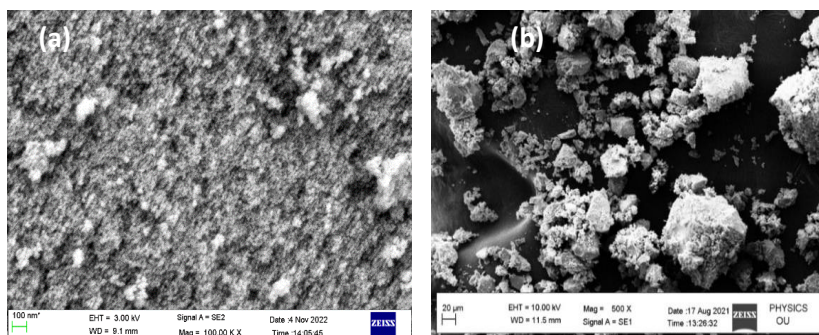


Figure 6: SEM micrographs of (a) TiO_2 and (b) $5\% \text{La}_2\text{O}_3\text{-TiO}_2$

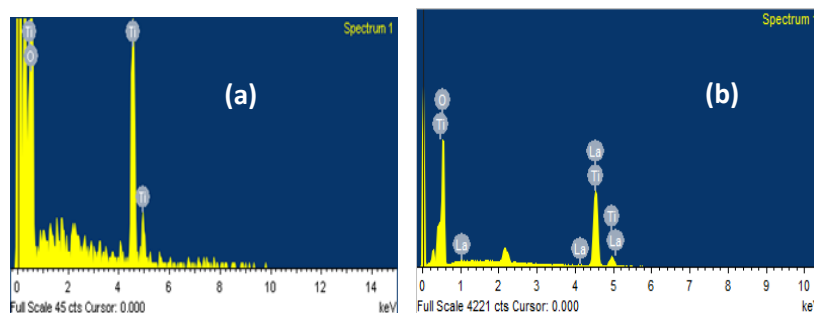


Figure 7: EDAX spectra and Elemental composition of (a) Nano TiO_2 and (b) $5\% \text{La}_2\text{O}_3\text{-TiO}_2$

Table 2: EDAX elemental composition of A) TiO₂ B) 5% La₂O₃-TiO₂

A) TiO ₂			B) 5% La ₂ O ₃ -TiO ₂		
Element	Weight %	Atomic %	Element	Weight %	Atomic %
O K	41.42	67.92	O K	41.71	68.48
Ti K	58.58	32.08	Ti K	57.06	31.29
TOTAL	100		La K	1.23	0.23
			TOTAL	100	

In the SEM analysis of 5% La₂O₃-TiO₂, distinct spherical shapes with nano-sized particles and minimal agglomeration were observed, indicating improved characteristics compared to nano TiO₂ as can be observed from figure 6 [5, 8]. Figure 7 and table 2 present the EDAX analysis that confirmed the presence of doped components in desired amounts. SEM micrographs depicted the morphology of Ti-La nanocomposites as independent of the La content. All samples exhibited spherical morphology resembling agglomerates of nano-sized particles, with a slight reduction in particle size observed with La doping. Elemental composition determined by Energy-dispersive X-ray spectroscopy (EDAX) supported XPS results [7].

TEM Analysis:

In terms of TEM analysis, the TEM image and particle size distribution in the figure 8 for the 5% La₂O₃-TiO₂ sample were provided. The mean size of the La doped TiO₂ was found to be 9.53 nm. The nanoparticles synthesized through the sol-gel method exhibited similar shapes but varied sizes. Pure TiO₂ nanoparticles had sizes ranging from 12-30 nm, while the 5% La-TiO₂ sample exhibited a distribution of about 8-20 nm with an average size of approximately 9.53 nm. The presence of La⁺³ in the doped TiO₂ samples led to a lower particle size distribution. These findings were consistent with the XRD results [8].

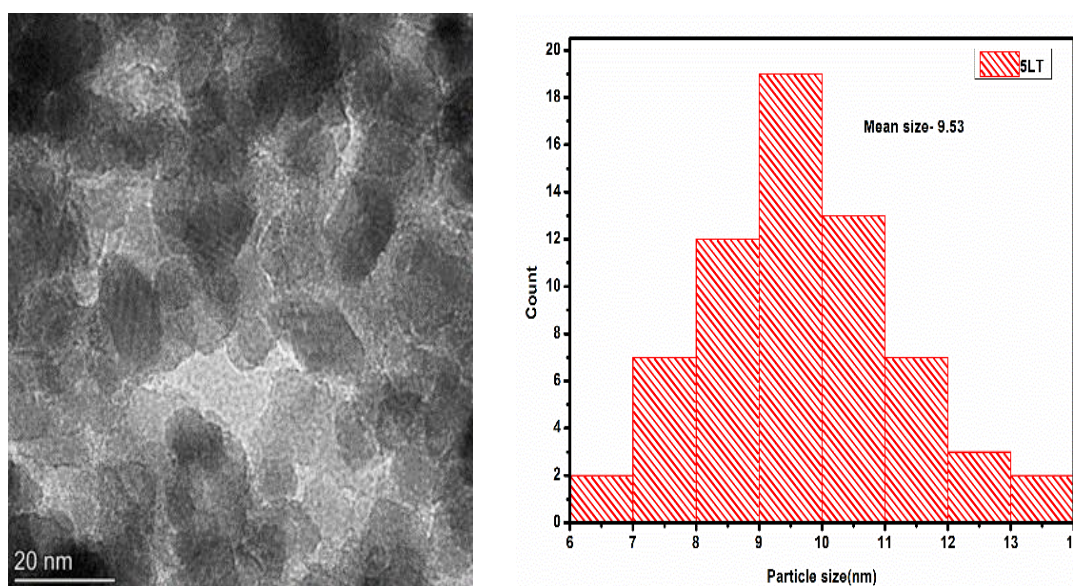


Figure 8: TEM image and particle size histogram of 5% La₂O₃-TiO₂

X-Ray Photoelectron Spectroscopy:

In the X-ray photoelectron Spectroscopy (XPS) analysis, the chemical states of elements in both pure TiO₂ and La-TiO₂ samples annealed at 500°C were examined. The XPS results are presented in Figure 9. Figure 9A displays the total spectra, revealing the presence of Ti and O elements in both pure TiO₂ and La-TiO₂ samples. Additionally, the appearance of the La 3d peak in the La-TiO₂ pattern indicated the presence of La due

to doping. The absence of La in the XPS spectrum may be due to the low La content falling below the limit of XPS detection.

High-resolution spectra of Ti 2p are shown in Figure 9B. In pure TiO₂, Ti 2p_{3/2} and Ti 2p_{1/2} peaks were observed at 458.3 eV and 464.2 eV, respectively, corresponding to Ti⁴⁺. Similarly, in La-TiO₂, Ti 2p_{3/2} and Ti 2p_{1/2} peaks were found at 458.5 eV and 464.5 eV, indicating a Ti⁴⁺ state in both cases. Figure 9D displayed the high-resolution La 3d spectrum. Peaks at 839 eV and 852 eV were because of La 3d_{5/2} and La 3d_{3/2}, respectively, signifying the presence of La as La⁺³ [8].

The XPS spectra of O 1s are depicted in Figure 9C. Peaks at 530.1 eV for pure TiO₂ and 529.8 eV for La-TiO₂ were attributed to O 1s. The Ti-O peak appeared at lower band gap energy due to the difference in electronegativity between the two elements.

These XPS results provided insights into the chemical states and compositions of the elements present in the pure TiO₂ [8].

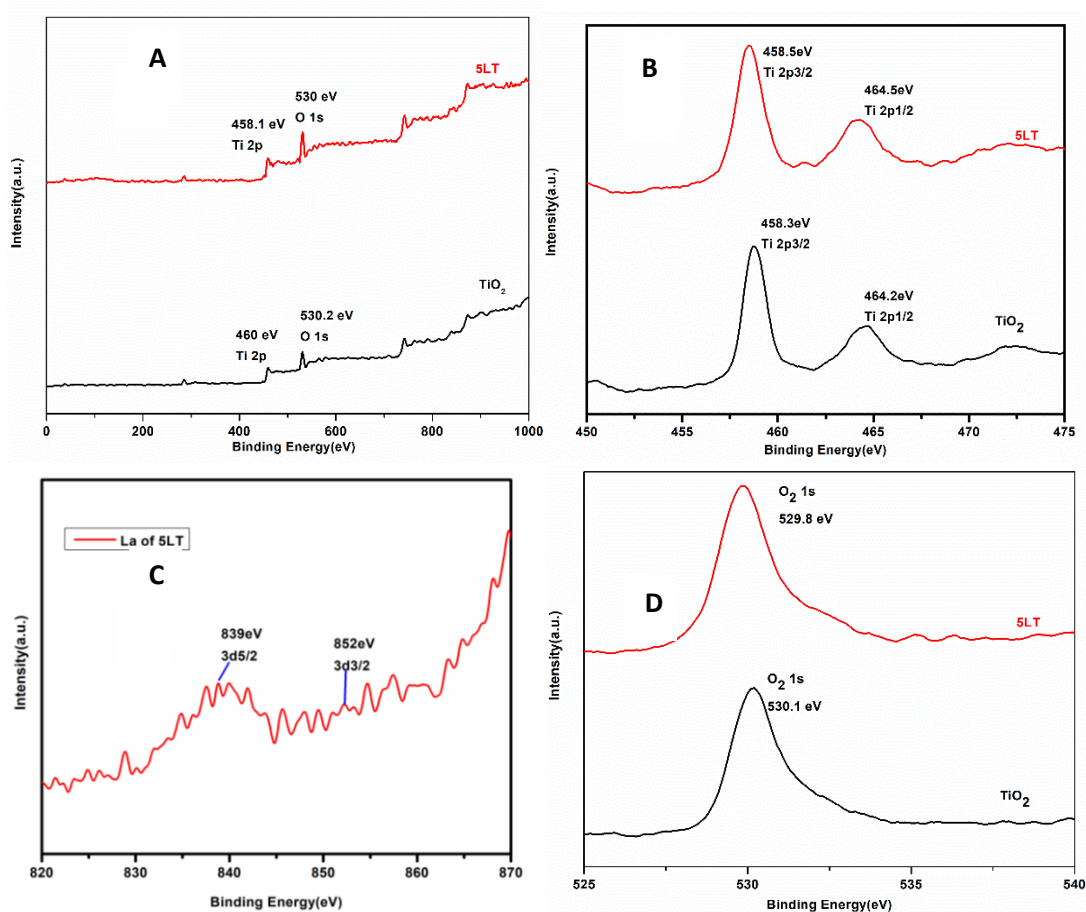


Figure 9: XPS spectra of TiO₂ and 5wt % La₂O₃-TiO₂, (A) Wide Scan (B) Ti 2p (C) La 3d (D) O 1s

Photo catalytic degradation:

The catalyst's performance under visible light was notably impressive. The 5% La₂O₃-TiO₂ nanocomposite exhibited high efficiency in degrading Acid Blue and Brilliant Yellow dyes, achieving degradation rates of 96% and 99%, respectively, which surpassed the results obtained with nano TiO₂ (Figures 10 and 11). A mere 75mg of the La-doped TiO₂ catalyst demonstrated a remarkable 99% degradation of 50 ppm Acid Blue dye (Figure 10B).

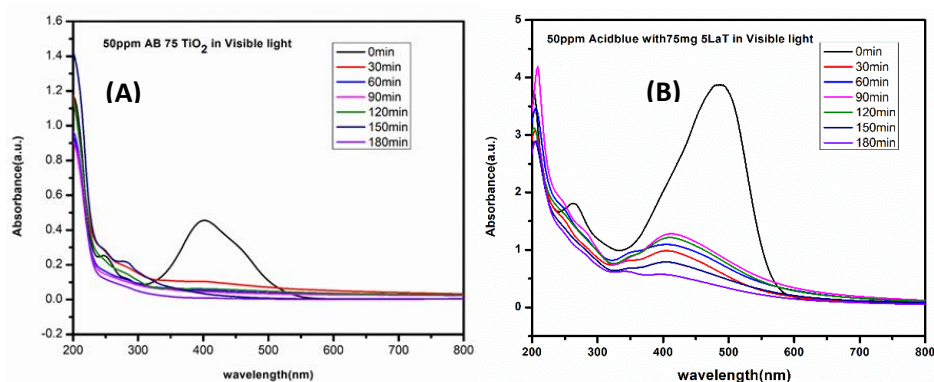


Figure 10: Photodegradation of 50 ppm Acid Blue using 75 mg catalyst in visible light over (A) Nano TiO₂ and (B) 5%La₂O₃-TiO₂ nanocomposite

The kinetics of dye degradation followed a Langmuir-Hinshelwood model with a first-order fit (Figures 13A & B), a pattern observed in other studies as well [11, 12]. The rate constants from table 3 for Brilliant Yellow dye were $1.6 \times 10^{-2} \text{ min}^{-1}$ for nano TiO₂ and $2.1 \times 10^{-2} \text{ min}^{-1}$ for 5% La₂O₃-TiO₂. For Acid Blue dye, the rate constants were $1.8 \times 10^{-2} \text{ min}^{-1}$ for nano TiO₂ and $2.2 \times 10^{-2} \text{ min}^{-1}$ for 5% La₂O₃-TiO₂, indicating the catalysts' high intrinsic activity. These results are correlated with the degradation efficiencies observed earlier.

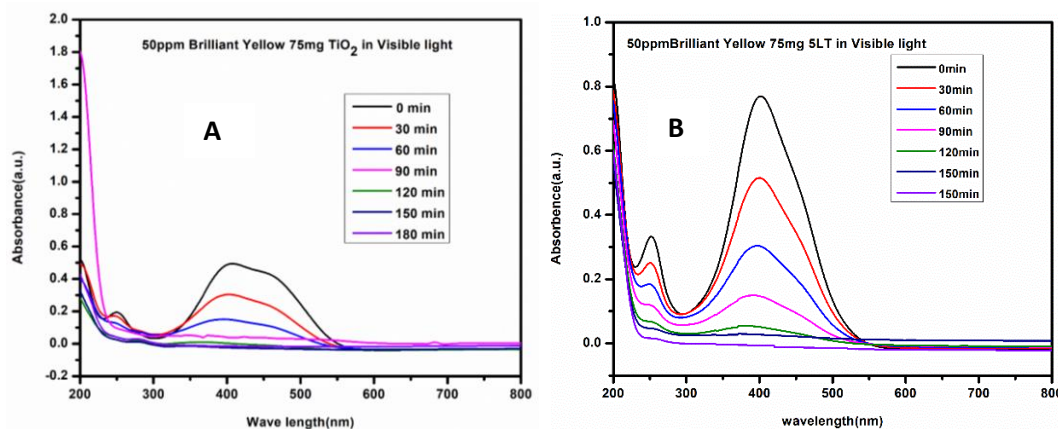


Figure 11: Photodegradation of 50 ppm Brilliant Yellow using 75 mg catalyst in visible light over (A) Nano TiO₂ and (B) 5%La₂O₃-TiO₂ nanocomposite

The comparison of Acid Blue and Brilliant Yellow dye degradation using La-doped TiO₂ particles and pure TiO₂ under air and sunlight conditions was presented in Figure 12. La-doped TiO₂ displayed superior photocatalytic activity, with degradation rates 12% higher for Brilliant Yellow dye and 13% higher for Acid Blue dye compared to pure TiO₂. This enhancement was attributed to an enhancement of anatase phase due to La doping, which aligns with increase in the photocatalytic activity of TiO₂.

Table 3: Rate constants of Photodegradation of Brilliant Yellow and Acid blue dyes

Catalyst	TiO ₂	5LT
Rate Constant of BY Degradation k (min ⁻¹)	1.6×10^{-2}	2.1×10^{-2}
Rate Constant of AB Degradation k (min ⁻¹)	1.8×10^{-2}	2.2×10^{-2}

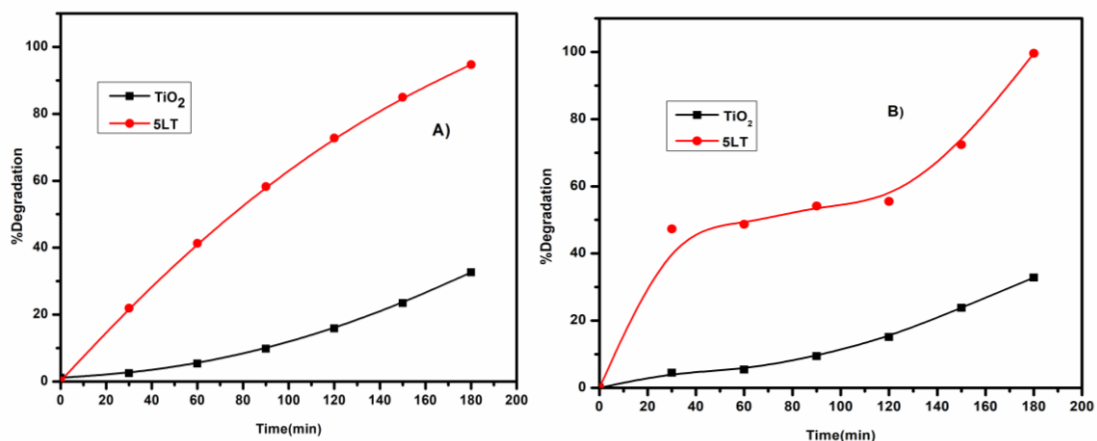


Figure 12: % Photodegradation of A) Brilliant Yellow B) Acid Blue in visible light over Nano TiO₂ and 5%La₂O₃-TiO₂ nanocomposite

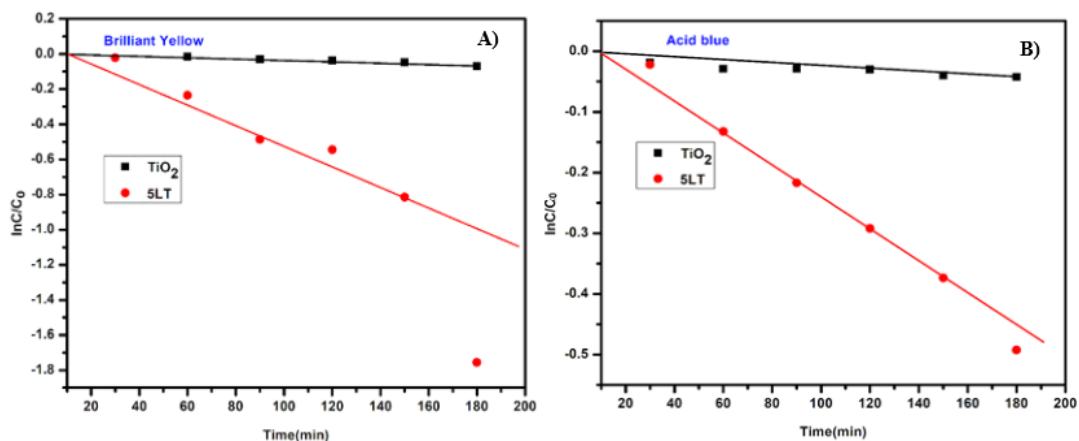


Figure 13: Kinetics of A) Brilliant Yellow B) Acid Blue in visible light over Nano TiO₂ and 5%La₂O₃-TiO₂ nanocomposite

Reusability of the catalysts:

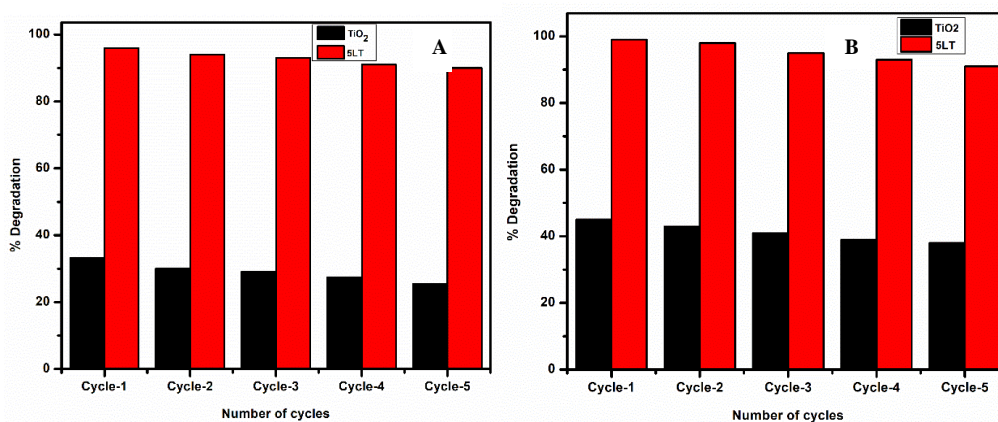
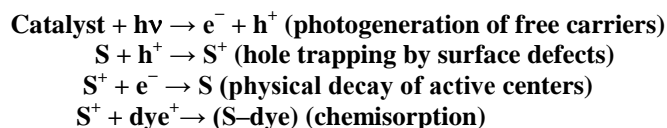
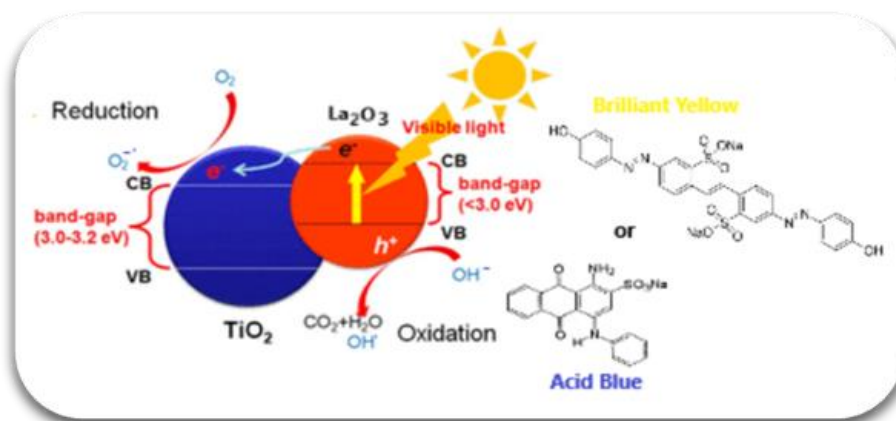


Figure 14: Reusability studies of Photodegradation of A) Brilliant Yellow B) Acid Blue in visible light over Nano TiO₂ and 5%La₂O₃-TiO₂ nanocomposite

The reusability studies were monitored for five cycles of run. Figure 14 shows the photocatalytic activity towards BY degradation decreased slightly from 96%-90% and towards AB degradation from 99%-92%. These results suggest good stability of the photocatalyst which remains unchanged even after five successive runs as also observed from used catalyst XRD analysis (not shown here).

Scheme of Reaction Mechanism:



In the photodegradation mechanism, when catalyst exposed to light radiation that generates the electron-hole pairs, which entrapped on the surface of catalyst, and interactions leading to the creation of superoxide and hydroxyl radicals [13]. These radicals further engage with the dye molecule, resulting in degradation. The presence of a dopant energy level within the band gap due to Lanthanum modification leads to a red shift in the absorption spectra, observed in UV-DRS spectra. Reduced recombination rates with TiO₂ modification by La contribute to the higher degradation rates achieved.

IV. CONCLUSIONS

The sol-gel synthesized nano TiO₂ and La₂O₃-TiO₂ nanocomposite demonstrated exceptional efficiency in the photocatalytic degradation of Brilliant Yellow and Acid Blue dyes. The nanocomposite, particularly, showcased higher efficacy for degrading elevated dye concentrations. The catalyst's nanocrystalline structure and spherical morphology were confirmed by XRD patterns and SEM images. A clear reduction in band gap from UV-DRS study and PL intensity reduction indicating a lowering recombination rate of e⁻-h⁺ pair explains the enhanced photocatalytic activity of the La-doped catalyst. Moreover, the catalyst maintained stable activity over five runs, confirming its efficiency as a visible-light degradation catalyst for the mentioned dyes.

CONFLICT OF INTEREST

The authors declared no conflict of interest.

ACKNOWLEDGEMENTS

The authors thank OU-DST-PURSE II and OU-UGC-SAP-DRS-II for the financial support and Prof. M. Vithal, Emeritus Scientist, University College of Science, Dept. of Chemistry, Osmania University, Hyderabad for allowing us to do this research work by utilizing his laboratory equipment. The authors also thank Dr A. Venugopal, Chief Scientist, CSIR-IICT and Dr L. Giribabu, Senior Principal Scientist, CSIR-IICT for the support extended in some of the characterization of catalysts.

REFERENCES

- [1]. J. Schneider, M. Matsuoka, M. Takeuchi, J.L. Zhang, Y. Horiuchi, M. Anpo, D.W. Bahnemann, Understanding TiO₂ Photocatalysis: Mechanisms And Materials. *Chem. Rev.* 114 (2014) 9919–9986.
- [2]. X. Chen, S.S. Mao, Titanium Dioxide Nanomaterials: Synthesis, Properties, Modifications, And Applications, *Chem. Rev.* 107 (2007) 2891–2959.
- [3]. N. Serpone, Is The Band Gap Of Pristine TiO₂ Narrowed By Anion- And Cation-Doping Of Titanium Dioxide In Second Generation Photocatalysts, *J. Phys. Chem. B* 110 (2006) 24287–24293.
- [4]. F. Wang.; Z.Z. Ma, P.P. Ban, X.H. Xu, C, N, And S Codoped Rutile TiO₂ Nanorods For Enhanced Visible-Light Photocatalytic Activity, *Mater. Lett.* 195 (2017) 143–146.
- [5]. K. Umar, M.M. Haque, M. Muneer, T. Harada, M. Matsumura, Mo, Mn And La-Doped TiO₂: Synthesis, Characterization And Photocatalytic Activity For The Decolorization Of Three Different Chromophoric Dyes, *Journal Of Alloys And Compounds.* 578 (2013) 431-438.
- [6]. B. Vijayalaxmi, Mamathasri, Ch.Vijayatha And A. Hari Padmasri, Photocatalytic Degradation Of Acid Alizarin – Violet N Dye In Visible Light Over Nano TiO₂ And Ag-Doped Nano TiO₂ Catalysts, *IOSR Journal Of Applied Chemistry* 15 (2022) 1-6.
- [7]. E. Borgarello, J. Kiwi, M. Gratzel, E. Pelizzetti And M. Visca, *J. Am. Chem. Soc.* 104 (1982) 2996-3002.
- [8]. Adriana Marizcal-Barba, Isaias Limón-Rocha, Arturo Barrera, José Eduardo Casillas, O. A. González-Vargas, José Luis Rico, Claudia Martínez-Gómez, Alejandro Pérez-Larios, TiO₂-La₂O₃ As Photocatalysts In The Degradation Of Naproxen, *Inorganics* 10(5) (2022) 67.
- [9]. K. Hashimoto, H. Irie, A. Fujishima, TiO₂ Photocatalysis: A Historical Overview And Future Prospects, *Japanese Journal Of Applied Physics* 44(12) (2005) 8269–85.
- [10]. Wen, Chen & Deng, Hua & Tian, Jun-Ying & Zhang, Ji-Mei. Photocatalytic Activity Enhancing For TiO₂ Photocatalyst By Doping With La, *Trans. Nonferrous Met. Soc. China* 16 (2006) S728-S731.
- [11]. A. Mills, R.H.Davies And D.Worsley, Waterpurification By Semiconductor Photocatalysis, *Chem. Soc. Rev.* 22 (1993); 417-425.
- [12]. Ioannis K. Konstantinou And Triantafyllos A. Albanis, TiO₂- Assisted Photocatalytic Degradation Of Azo Dyes In Aqueous Solution: Kinetic And Mechanistic Investigations; A Review, *Applied Catalysis B: Environmental*, 49 (2004) 1–14.
- [13]. B. Neppolian, S. Sakthivel, B. Arabindoo, M. Palanichamy, And V. Murugesan, Degradation Of Textile Dye By Solar Light Using TiO₂ And ZnO Photocatalysts, *Journal Of Environmental Science And Health Part A., Toxic/Hazardous Substances And Environmental Engineering*, 34(9) (1999) 1829-1838.